

Photo-induced switching of microwave and millimeter-wave signals on coplanar waveguides

G. Koers¹, G. Poesen¹, P. Simon², J.-P. Raskin², J. Stiens¹, I. Huynen², R. Vounckx¹

¹ Vrije Universiteit Brussel, Lab for Micro- and Optoelectronics, Pleinlaan 2,
B-1050 Brussels, Belgium.

² Université catholique de Louvain, Microwave Laboratory, Place du Levant 3,
B-1348 Louvain-la-Neuve, Belgium

An optically generated plasma can induce local changes in the dielectric properties of a semiconductor substrate carrying the coplanar waveguide transmission line in order to switch the propagating millimeter waves. Different transmission line layouts have been implemented to optimize the electromagnetic field configuration and to enhance the interaction between the infrared excitation and microwave and millimeter wave signal. Practical design steps are discussed and experimental results of insertion and reflection losses of CPW on GaAs and Si substrates are presented from 40 MHz up to 40 GHz at an excitation wavelength of 785 nm.

Introduction

At millimetre-wave frequencies, novel imaging methods offer a large potential in security applications. In active imaging systems, an artificial radiation source is employed to illuminate the scene under observation. This approach increases the attainable image contrast in indoor environments with several orders of magnitude. However, image quality suffers because simple artificial millimetre-wave sources are highly coherent. A new approach to the design of a non-coherent illumination source is the introduction of a scattering surface with resonating antenna elements which acts as a secondary light source with tunable characteristics. Sub-areas on this reflecting surface should scatter with time-varying and random phase-shifts in order to create a non-coherent light source suitable for imaging. Practically, this can be achieved by antennas coupled and loaded with variable impedances. For the design of such impedances we require:

- 1) impedance switching at relatively low frequencies (< MHz)
- 2) hybrid integration on antenna substrate
- 3) scalability of control circuit (up to several hundreds of elements)

Taking into account these requirements, opto-electronic control of microwave circuits could turn out to be an interesting alternative to discrete device switching with FETs or PIN-diodes. Simple photodetection-based devices could be less expensive compared to overqualified integrated circuits and better galvanic separation offers a larger degree of design freedom at the level of control circuitry. Coplanar waveguides are used intensively for millimeter-wave coupling and propagation on planar dielectric substrates and we therefore choose this structure to verify and illustrate our ideas. Optically induced losses on CPWs have already been illustrated up to 20 GHz in [1] and for open terminated microstrip lines up to 40 GHz in [2].

Device modeling

A useful approach to model the process of free carrier generation in a semiconductor substrate is to approximate the active region by a region with increased conductivity, calculated from the incident optical power. We use the formulas obtained from the rigorous quasi-static analysis for coplanar waveguides as presented in [1] to calculate the effective photoconductivity $\Delta\sigma_m$ and plasma penetration depth d_e .

$$\Delta\sigma_m = \frac{\Delta\sigma_0}{1 + \alpha_r L_a} \left[\frac{1}{\alpha_r L_a} \left(\frac{\alpha_r L_a^2 + v_s \tau}{L_a + v_s \tau} \right) \right]^{-\alpha_r L_a / (1 - \alpha_r L_a)} \quad (1)$$

$$d_e = \frac{1}{\alpha_r} \left[\frac{(1 + \alpha_r L_a) L_a + v_s \tau}{L_a + v_s \tau} \right] \left[\frac{1}{\alpha_r L_a} \left(\frac{\alpha_r L_a^2 + v_s \tau}{L_a + v_s \tau} \right) \right]^{\alpha_r L_a / (1 - \alpha_r L_a)} \quad (2)$$

Here $\alpha_r(\lambda)$ is the absorption coefficient, v_s is the surface recombination velocity, τ is the excess carrier lifetime, $\Delta\sigma_0$ is the photoconductivity at the air-semiconductor interface and L_a is the ambipolar length, both given by

$$\Delta\sigma_0 = \frac{q}{hc_0} (\mu_n + \mu_p) (1 - R) \alpha_r S \lambda_p \tau \frac{P}{A} \quad (3)$$

$$L_a = \sqrt{\frac{2 \mu_n \mu_p \tau k_B T}{q (\mu_n + \mu_p)}} \quad (4)$$

Where q is the unit electronic charge, h is Planck's constant, c_0 is the speed of light in vacuum, μ_n and μ_p are the electron and hole mobilities, $R(\lambda)$ is the surface reflectivity, $S(\lambda)$ is the relative spectral response of the semiconductor material exhibiting a peak response at the optical wavelength λ_p , τ is the excess carrier lifetime, P is the optical power and A is the illuminated area, k_B is Boltzmann's constant, T is the absolute temperature. The internal quantum efficiency of the semiconductor is assumed to be unity, which correspond to perfectly intrinsic photogeneration. The carrier lifetime and mobility are assumed independent of excess carrier density.

These calculated values can now be used in FDTD simulation. Relevant material properties and calculation results for our case are shown in Tables 1 and 2.

Spot size [mm ²]	Illumination Intensity [mW/mm ²]	Effective Intensity [mW/mm ²]	Active area [mm ²] (thru-line)	Effective Incident Power [mW]	σ_m for GaAs [S/cm]	σ_m for Si [S/cm]
0.4 x 0.3	405	283.5	0.013	5.35	98.8	489
0.2 x 0.15	1698	1188.6	0.007	11.21	410.0	2050

Table 1: Calculated photo-conductivities on GaAs and Si from Equation (1)

	Carrier lifetime [s]	α ($\lambda=785\text{nm}$) [cm^{-1}]	surface recombination velocity [cm/s]	Plasma penetration depth d_e [cm]
GaAs	10^{-8}	10^4	10^5	6.38×10^{-1}
Si	10^{-6}	10^3	10^3	5.4×10^{-3}

Table 2: Calculated plasma penetration depth on GaAs and Si from Equation (2)

Measurement set-up

The CPW transverse line dimensions were $26 \mu\text{m}$ (central conductor width) and $22 \mu\text{m}$ (slotwidth). Identical CPW designs were used on GaAs, Si, and high resistivity Silicon (HR-Si) substrates. The optical illumination source was a 785 nm laser with 45 mW maximum output power. The laser is focused through a standard microscope objective (4x). The elliptical spot is visually aligned to the CPW by means of a CCD camera coupled through a beamsplitter. The greatest difficulty we faced was the focusing of the spot, because the image focal was several mm from the spot focal. Therefore the minimal spotsize attained was in the order of $200 \mu\text{m} \times 150 \mu\text{m}$ (taking into account the lens aperture). Microwave measurements were performed with a Vector Network Analyzer (VNA) in the frequency range from 40 MHz to 40 GHz.

Experimental results

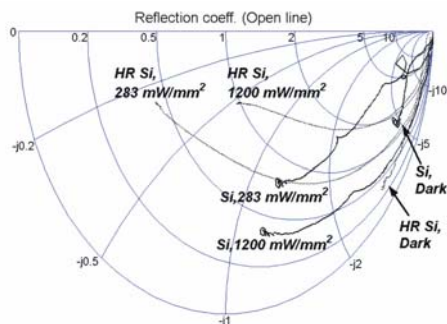


Fig.1: Measured reflection coefficient for open terminated CPW on Si and HR Si, illuminated with $283 \text{ mW}/\text{mm}^2$ and $1200 \text{ mW}/\text{mm}^2$.

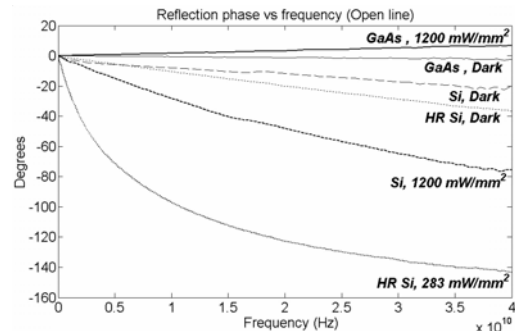


Fig.2: Measured reflection phase vs. frequency for open terminated CPW on Si, HR Si and GaAs illuminated with $283 \text{ mW}/\text{mm}^2$ and $1200 \text{ mW}/\text{mm}^2$.

From the measured data shown in Figures 1 and 2 it is seen that the reflection response on an open terminated CPW line, illuminated at the termination shows large contrast between no and strong illumination ($1200 \text{ mW}/\text{mm}^2$ on Si and $283 \text{ mW}/\text{mm}^2$ on HR-Si).

For HR-Si, the impedance magnitude at 40 GHz changes from a near open to about 25Ω and a phase difference of more than 100° was measured. The response for GaAs is much less pronounced, as expected due to its very short free carrier lifetime. Similar trends are visible in thru-line measurements (Figures 3 and 4 (only one port is shown for clarity)), where it is seen that reflection at the input port increases dramatically with two orders of magnitude

from around 30 dB to 5 dB and insertion loss increases around 6 dB to 8 dB from 20 GHz on. It must be noted that no de-embedding of input-mismatch at the probe contacts has been

performed on these results; this should explain the offset measured for the insertion loss of about 1 dB.

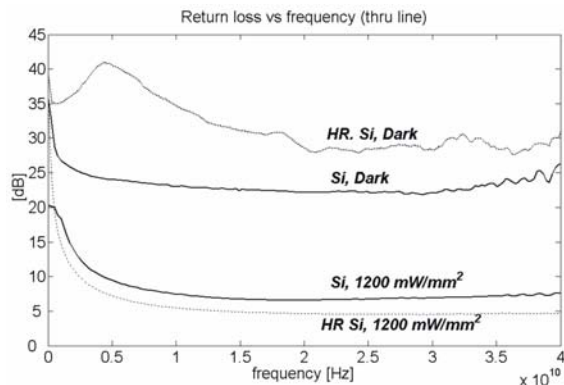


Fig. 3: Measured thru line return loss vs. frequency on Si and HR Si.

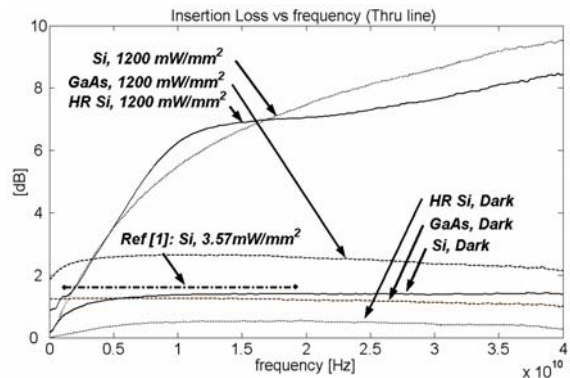


Fig. 4: Measured thru line insertion loss vs. frequency on Si, HR Si and GaAs. Data from [1] is added for reference.

Conclusions

Measured results up to 40 GHz show promising results for opto-electronic switching on coplanar waveguides on silicon substrates. Open ended and thru CPW lines exhibit strong illumination dependent behaviour and could be used for slow (< MHz) magnitude or phase-shifting applications. We are aware that the optical power needed for these effects is very large, but we think that a 50% efficiency increase could be achieved, first of all by reducing the reflection at the substrate-air interface, which accounts for about 30% of intensity loss and secondly by using better focusing and employing micromachining techniques. Interesting to note also is that the measured results become more pronounced at higher frequencies.

Acknowledgements

This work was partially funded by the Vrije Universiteit Brussel (VUB-GOA: Photonics in Computing-II, VUB-OZR), the Flemish Fund for Scientific Research (FWO- G.0071.02) and the European Union (IST-V Nefertiti).

References

- [1] W. Platte and B. Sauerer, Optically CW-induced losses in semiconductor coplanar waveguides. IEEE Transactions on microwave theory and techniques, Vol. 37, No. 1, pp139-148, January 1989.
- [2] M. Serres, Optical control of microwave planar devices on semiconductor substrate. Thèse présentée en vue de l'obtention du grade de docteur en Sciences Appliquées, Université Catholique de Louvain Laboratoire d'hyperfréquences. Décembre 1999.